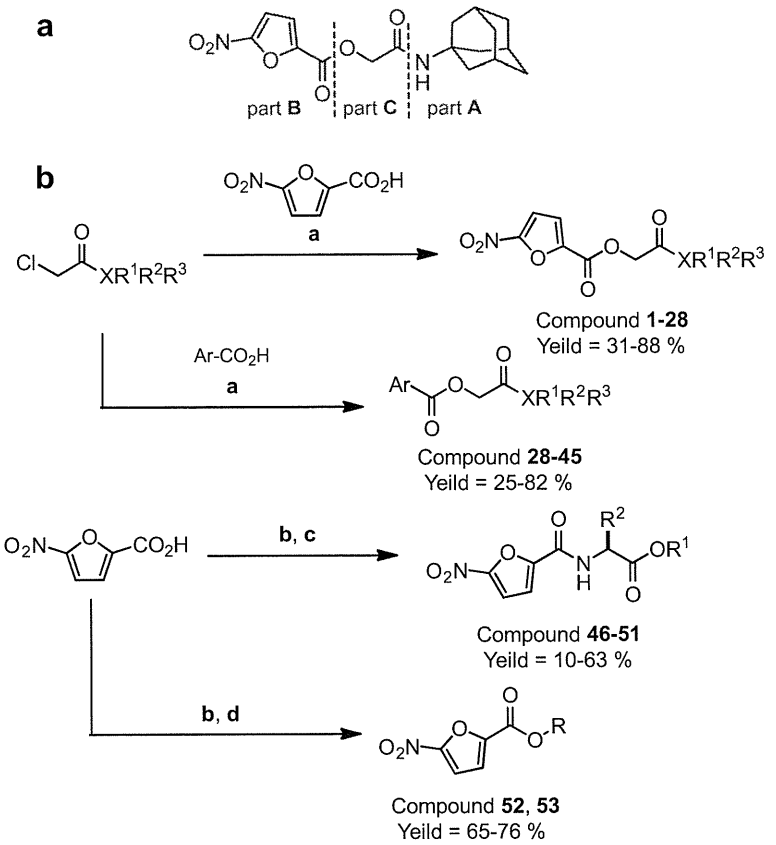

Figure 1. (a) Structure of a hit chemical showing RNase H inhibitory activity found in our previous in vitro screening. (b) Scheme for synthesis of the derivatives from the hit chemical. Eqs. 1, 2 and 3 correspond to the reactions for modulating parts A, B and C in (a), respectively. Eq. 4 indicates the reaction modulating the moiety connected to the ester bond at parts A and C.

lyzed against a buffer of 50 mM Tris–HCl at pH 7.5 and 200 mM NaCl and was stored at −20 °C with adding 50% (v/v) glycerol.

The inhibitory activities of synthesized compounds were measured by an enzymatic assay in a manner similar to that in the previous studies.[17,21,22] In short, a real-time monitoring assay was applied. For substrate, two oligo-nucleotides were annealed at final concentrations of 2.5 and 0.25 μM. One was oligo-ribonucleotide 5′-GAUCUGAGCCUGGGAGCU-3′ with 6-carboxy-fluoroscein (FAM) conjugated at the 3′ end, and the other was oligo-deoxyribonucleotide 5′-AGCTCCCAGGCTCAGATC-3′ with black hole quencher (BHQ) conjugated at the 5′ end. Enzyme reaction with 100 ng RT, 0.025 μM oligo-ribonucleotide, and 0.25 μM oligo-deoxyribonucleotide was carried out in a volume of 10 μL at 37 °C. Fluorescence at 488 nm was monitored every 150 s using a multimode detector.

2.3. Assessment of cytotoxicity

Cytotoxicity of the synthesized compounds was tested by an MTT assay with the celltiter 96 non-radioactive cell proliferation assay system (Promega). Two cell lines, MT-4 and 293T, were used in this assay. The cytotoxic assay was performed by the following 8-step procedure. (1) 100 μL RPM-1640 medium supplemented with 10% FBS containing 2% DMSO was loaded in a 96-well plate, and the outside of the wells was soaked with 100 μL PBS to prevent an edge effect. (2) 200 μL RPM-1640 medium with 10% PBS and 2% DMSO containing test compounds at a concentration of 200 μM was added to the wells in the first column of the plate. The final concentration of the compounds in these wells was 100 μM when cells were cultured. (3) A sequence of wells with different compound concentrations was prepared for the second, third and fourth columns. The final concentrations of these columns were 50, 25 and 12.5 μM. The wells in the fifth column were used for a control without adding any test compounds. (4) 100 μL MT-4 cells at a concentration of 4×10^5/mL or 100 μL 293T cells at a concentration of 2×10^5/mL was added to the respective wells. The final concentration of DMSO in each well was 1%. (5) Cells were incubated for 3 days at 37 °C with 5% CO_2 atmosphere. (6) 100 μL of supernant of the cultured medium was removed. Then 15 μL MTT reagent for dye solution was added to each well and the cells were incubated for 1 h. (7) 100 μL solution of solubilization and stop mix was added, and the cells were incubated overnight at 4 °C to sufficiently dissolve the dye. (8) Intensity of $OD_{570/690}$ was measured by a spectrofluorometer, BIO-TEK ELx808. Drug concentration showing 50% cell cytotoxicity was calculated only if the viability of cells was below 50% in the presence of compound at 100 μM.

2.4. Theoretical computation

A computational model of the target protein was constructed from an X-ray crystal structure of the RNase H domain of HIV-1 RT: 3HYF.[6] According to the results of the recent X-ray crystallographic studies on the complex of RNase H domain and chemical compounds showing RNase H inhibitory activity,[6–8] the RNase H

domain contains two Mn^{2+} ions at the center of the active site. Hence, two Mn^{2+} ions in the crystal structure were replaced with Mg^{2+} ions. The protonation states of all the ionasable residues were predicted by ProPKa program[23] in the presence of two Mg^{2+} ions at the active site. The prediction indicated deprotonation of Asp443, Glu478, Asp498, and Asp549. Chemical structures of the active compounds were built by using GaussView software, and geometry optimization was executed at the B3LYP/6-31G(d,p) level. Each compound was manually placed at the active site of RNase H domain. A quantum mechanical and molecular mechanics (QM/MM) approach was applied,[24] utilizing the ONIOM method of GAUSSIAN 03 program.[25] In our preliminary computations, molecular dynamics simulation hardly gave a reasonable binding conformation, because the RNase H domain contained divalent metal ions at the active site and the parameterization would be insufficient to reproduce the six-fold coordination of divalent metal ions. In QM/MM calculation, Asp443, Glu478, Asp498, Asp549, His539, compound, and two Mg^{2+} ions were set to the QM layer, and the other residues were set to the MM layer. No water molecules were included in the calculation model. Models including surrounding water molecules had also been examined in our preliminary trials of QM/MM calculation. Geometry optimization was hardly completed in the water-included models because of the difficulty in meeting the convergence criteria, in which even slight forces on atoms caused large displacements of the surrounding water molecules. Molecular orbitals in the QM layer were calculated at the B3LYP/6-31G(d,p) level and the universal force field was applied to the atoms in the MM layer. Geometry optimization was executed without any constraints to any atoms.

3. Results

Two hit chemicals, which were found in our previous in vitro screening, contain a nitro-furan ring and amide group bonding to

Table 1
Structure and RNase H inhibitory activity of the derivatives modulated at part A

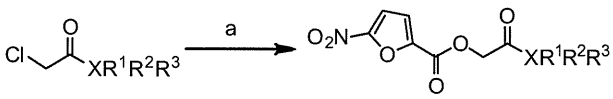

Compound **1-28**
Yeild = 31-88%

Conditions ; (a) 5-Nitro-2-furoic acid, DMAP, DMF, 80 °C, 6 h

Compound	X	R^1, R^2, R^3	Yield (%)	IC_{50} (μM)
1	O	R^1 = *i*-Pr	64	13.2
2	N	R^1 = H, R^2 = *t*-Bu	58	18.0
3		R^1 = H, R^2 = CMe_2Et	48	5.8
4		R^1 = H, R^2 = CMe_2Ph	43	8.2
5		R^1 = H, R^2 = CMe_2CH_2Ph	48	4.3
6		R^1 = H, R^2 = $CH_2CH(CH_2)_3O$	64	4.2
7		R^1 = H, R^2 = 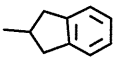	59	5.5
8	N	R^1 = H, R^2 = 	38	6.1
9		R^1 = H, R^2 = 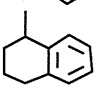	45	4.3
10	N	R^1 = *t*-Bu, R^2 = CH_2Ph	82	0.9
11		R^1 = *t*-Bu, R^2 = CH_2CH_2Ph	74	14.2
12		R^1 = *t*-Bu, R^2 = $CH_2(CH_2)_2Ph$	82	>50
13		R^1 = *t*-Bu, R^2 = $CH_2CH_2C(O)Ph$	88	>50
14	N	R^1 = *t*-Bu, R^2 = CH_2*p*-$NO_2C_6H_4$	72	6.9
15		R^1 = *t*-Bu, R^2 = CH_2*m*-$NO_2C_6H_4$	69	9.8
16		R^1 = *t*-Bu, R^2 = CH_2*p*-$AcOC_6H_4$	45	8.7
17		R^1 = *t*-Bu, R^2 = CH_2*o*-$AcOC_6H_4$	31	12.8
18		R^1 = *t*-Bu, R^2 = CH_2*p*-$MeOC_6H_4$	68	7.5
19		R^1 = *t*-Bu, R^2 = CH_2*p*-$BnOC_6H_4$	73	>50
20	N	R^1 = *t*-Bu, R^2 = CH_2*p*-FC_6H_4	64	8.5
21		R^1 = *t*-Bu, R^2 = CH_2*p*-$CF_3C_6H_4$	71	8.0
22		R^1 = *t*-Bu, R^2 = CH_2*m*-$CF_3C_6H_4$	69	8.5
23		R^1 = *t*-Bu, R^2 = CH_2*o*-$CF_3C_6H_4$	72	9.0
24		R^1 = *t*-Bu, R^2 = $CH_2$2,3,4,5,6-F_5C_6	68	6.8
25	N	R^1 = $CH_2CH(CH_2)_3O$, R^2 = CH_2Ph	32	7.7
26		R^1 = $CH_2CH(CH_2)_3O$, R^2 = CH_2*p*-HOC_6H_4	45	5.0
27	C	R^1 = H, R^2 = H, R^3 = H	56	7.1
28		R^1 = Me, R^2 = Me, R^3 = Me	49	21.9

Conditions: (a) 5-nitro-2-fuloric acid, DMAP, DMF, 80 °C, 6 h.

a hydrophobic substitute. The nitro-furan ring is connected to the amide group through an ester linkage. Synthesis of these chemicals was accomplished by coupling reaction of nitro-furoic acid with α-chloro carbonylate containing of a hydrophobic substitute and an amide group. Hence, three series of analogue compounds were synthesized by the following strategy for modulating parts A, B and C of Figure 1a: (A) conversion of the hydrophobic substitute bound to the amide group to other substitutes, (B) conversion of the nitro-furan ring to several other chemical structures, and (C) conversion of the ester linkage to an amide bond.

The 50% inhibitory concentration (IC_{50}) of the compounds for HIV-1 RT-associated RNase H activity was determined from the chemical concentration leading half the rate for substrate cleavage reaction relative to the control. A real-time monitoring assay was carried out to estimate IC_{50} of the synthesized compounds.

As shown in Table 1 and 28 analogues were synthesized by converting the hydrophobic substitute at part A. In the in vitro assay for inhibitory activity, most of the analogues exhibited a similar degree of inhibitory potency to the hit chemical in Figure 1a, the IC_{50} value of which was 16.5 μM. Inhibitory activity was retained with conversion of the amide bond to an ester linkage and substitution of the hydrophobic region with *iso*-propyl (**1**). A set of derivatives containing two methyl groups and one hydrophobic substitute such as *t*-butyl, pentyl or phenyl bound to an alkyl carbon connecting to the amide group was surveyed (**2**–**5**). Substitution of tetrahydrofuran was also tested (**6**). These derivatives had similar potencies. In particular, tetrahydrofuran substitution (**6**) increased compound potency by approximately fourfold from the hit chemical. The effect of introduction of a phenyl group was examined in two forms: one is through connection with cyclo-carbons

Table 2
Structure and RNase H inhibitory activity of the derivatives modulated at part B

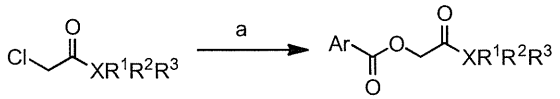

Compound **28-45**
Yeild = 25-82%
Conditions ; (a) Ar-CO_2H, DMAP, DMF, 80 °C, 6 h

Compound	X	Ar-CO_2H	R^1, R^2, R^3	Yield (%)	IC_{50} (μM)
29	N	*o*-Nitro-$C_6H_4CO_2H$	R^1 = H, R^2 = *t*-Bu	57	>50
30		*m*-Nitro-$C_6H_4CO_2H$	R^1 = H, R^2 = *t*-Bu	60	>50
31		*p*-Nitro-$C_6H_4CO_2H$	R^1 = H, R^2 = *t*-Bu	49	>50
32		3,5-Dinitro-$C_6H_3CO_2H$	R^1 = *t*-Bu, R^2 = CH_2Ph	34	>50
33		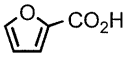	R^1 = *t*-Bu, R^2 = CH_2Ph	67	>50
34	N	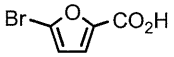	R^1 = H, R^2 = *t*-Bu	30	>50
35		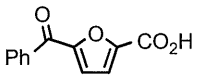	R^1 = H, R^2 = *t*-Bu	43	>50
36	N	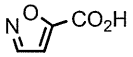	R^1 = H, R^2 = *t*-Bu	25	>50
37		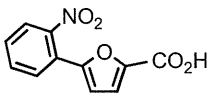	R^1 =H, R^2 = *t*-Bu	82	>50
38	N	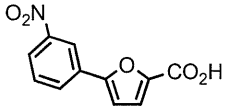	R^1 = H, R^2 = *t*-Bu	61	>50
39		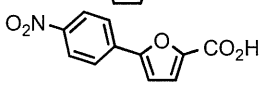	R^1 =H, R^2 = *t*-Bu	46	>50
40		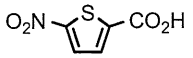	R^1 = H, R^2 = *t*-Bu	61	2.8
41	N	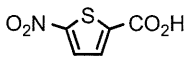	R^1 = H, R^2 = CMe_2Et	32	5.8
42		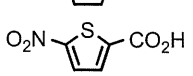	R^1 = CMe_2Et, R^2 = CH_2*p*-NO_2C_6H	58	33.5
43		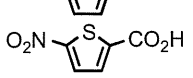	R^1 = CMe_2Et, R^2 = CH_2*m*-$NO_2C_6H_4$	64	25.8
44	C	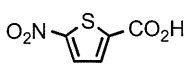	R^1 = H, R^2 = H, R^3 =H	56	9.5
45		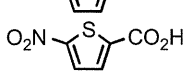	R^1 = Me, R^2 = Me, R^3 =Me	48	5.7

Conditions: (a) Ar-CO_2H, DMAP, DMF, 80 °C, 6 h.

(**7–9**) and the other with an alkyl chain (**10–13**). A highly potent compound (**10**) was found in the analogues in which a benzyl group with a *t*-butyl substitute was introduced. This derivative (**10**) showed an 18-fold increment of RNase H inhibitory activity from the original hit chemical. In contrast, no inhibitory activity was observed for the analogues with a phenyl group introduced via more than two chain atoms of carbon or oxygen (**12** and **13**). The effect of introduction of a phenyl group via an alkyl chain was further examined by connecting some polar functional groups, nitro, acetyl, methoxy and phenoxy, to the phenyl (**14–19**). These derivatives showed inhibitory activities similar to that of the hit chemical, while no activity was observed only for the connection of phenoxy (**19**), which was a considerably large substitute. The introduction of fluoride was examined with the phenyl group linked to an amide bond via an alkyl chain (**20–24**). These derivatives exhibited similar degrees of inhibitory activity, but no highly potent compound was found with fluoride introduction. The introduction of tetrahydrofuran with a benzyl or hydroxy benzyl group (**25** and **26**) was examined. Both compounds showed inhibitory activity similar to that of the hit chemical. The amide group was converted to a carbonyl group (**27** and **28**). A similar degree of inhibitory activity was maintained with conversion of the amide bond to an acetyl group, while conversion to oxy *t*-butyl decreased the inhibitory potency.

As shown in Table 2 and 17 analogues were synthesized by converting the nitro-furan ring at part B into other ring structures. Most of the analogues lost inhibitory potency for RNase H enzymatic activity or had significantly reduced inhibitory activity. Conversion of the furan ring into benzene (**29–32**) resulted in loss of compound potency, regardless of the location of the nitro group at the *orto*-, *meta*- or *para*-position. The derivative containing two nitro groups (**32**) also showed no inhibitory activity. A series of derivatives with modification of the nitro group (**33–36**) exhibited no inhibitory activity. Removal of the nitro group (**33**), replacement by bromide (**34**), replacement by carbonyl phenyl (**35**), or removal of even hydrogen (**36**) resulted in complete loss of compound potency. Substitution of the nitro group by nitro-benzene (**37–39**) resulted in no inhibitory activity regardless of the position of the nitro group bonding to benzene. Substitution of the furan ring with thiophene (**40–45**) was surveyed. Some derivatives were more potent than the hit chemical. An analog derived from compound **3** with conversion of the furan ring into thiophene (**40**) showed high inhibitory activity.

As shown in Table 3 and six analogues were synthesized by exchanging the ester bond at part C. Ester linkage is disadvantageous for medicine because esterase digests the linkage and the drug concentration in a body is rapidly decreased. The ester linkage was replaced by an amide group (**46–51**). None of the derivatives showed noticeable inhibitory activity.

As shown in Table 4 and two analogues were synthesized by converting the region connected to the ester bond at parts A and C. Both derivatives (**52** and **53**) increased compound potency 6–8-fold from the hit chemical. It is interesting to note that the distance from the ring part of the substituted moiety to the ester bond is small compared to a series of derivatives listed in Table 1.

In the measurement of cytotoxicity using MT-4 cells, almost all chemical compounds showed no cytotoxicity at a concentration of 100 μM, except for compounds **21**, **23**, **52** and **53** as shown in Table 5. In the measurement using 293T cells, many compounds showed no noticeable cytotoxicity at a concentration of 100 μM, while seven compounds, **11**, **15**, **21**, **22**, **23**, **24** and **52** showed cytotoxicity in which CC_{50} ranged from 36 to 83 μM. Compounds showing cytotoxicity contain several fluoride atoms (**21–24**). Cytotoxicity was also observed in a compound bearing a nitro-benzyl group (**15** and **52**), which is a chemical structure known as a cause for genotoxicity. Overall, the assessment of cytotoxicity suggested

Table 3
Structure and RNase H inhibitory activity of the derivatives modulated at part C

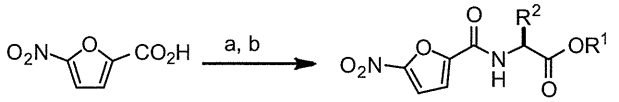

Compound **46-51**
Yeild = 10-63%

Conditions ; (a) $SOCl_2$, CH_2Cl_2, reflux, 3 h,
(b) Aminoacidester, NEt_3, CH_2Cl_2, 0 °C-rt, 1 h

Compound	R^1, R^2	Yield (%)	IC_{50} (μM)
46	R^1 = Me, R^2 = H	10	>50
47	R^1 = Et, R^2 = Me	70	>50
48	R^1 = Et, R^2 = CH_2i-Pr	45	>50
49	R^1 = Et, R^2 = CH_2Ph	60	>50
50	R^1 = Et, R^2 = CH_2p-OHC_6H_4	63	>50
51	R^1 = Et, R^2 = Ph	61	>50

Conditions: (a) $SOCl_2$, CH_2Cl_2, reflux, 3 h; (b) amino acid ester, NEt_3, CH_2Cl_2, 0 °C to rt, 1 h.

that a nitro-furan core has little cytotoxicity for MT-4 and 293T cells and that the scaffold tested in this study is favorable from a cytotoxic viewpoint. It is notable that there is some degree of difference in concentrations of compounds showing noticeable cytotoxicity between MT-4 and 293T cells.

4. Discussion

Two hit chemicals found in our previous in vitro screening bear an ester linkage at the connection of the nitro-furan group and the hydrophobic moiety.[17] All of the compounds showing RNase H inhibitory activity in Tables 1 and 2 have this ester linkage. Table 3 clearly indicates that conversion of the ester linkage into an amide bond results in loss of inhibitory potency. The amide bond is likely to form a planar configuration. Hence, a straight form is favorable for the amide linkage of nitro-furan and the hydrophobic moiety. If a compound has a straight form, the side part of the compound will collide with the inside wall of the binding pocket of the RNase H domain. Accordingly, it will be difficult for the compound to combine with the binding pocket. This suggests that an amide bond adjacent to the nitro-furan group is unfavorable for RNase H inhibitors.

As shown in Table 1, no drastic change was observed in inhibitory activity when the hydrophobic moiety connecting to carbonyl carbon was substituted by various kinds of chemical groups. This indicates that the substituted region has little interaction with the RNase H domain, suggesting that the substituted region will be located outside the binding pocket and exposed to the solvent. This indicates that a strategy for increasing inhibitory activity is for the position of the substitute to be closer to the nitro-furan group or instead more distant from it. The former conversion may make the aromatic ring or hydrophobic substitute interact with the target protein inside the binding pocket. The latter will make the substitute interact with a neighboring hollow site outside the binding pocket.

Table 2 shows that conversion of the nitro-furan group into other chemical structures drastically decreases the inhibitory activity except for nitro-thiophen. This means that a nitro-furan core is indispensable for inhibitory potency induced by analogues of the hit chemical in Figure 1a. The characteristic property of nitro-furan is large electric polarity. Oxygen atoms are negatively charged. These oxygen atoms will be coordinated to divalent metal ions at the RNase H active site. Accordingly, enhancing the

Table 4
Structure and RNase H inhibitory activity of the derivatives modulated at the moiety connected to the ester bond in parts A and C

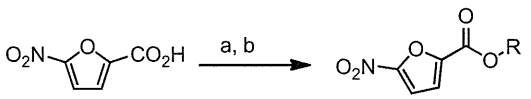

Compound **52**,**53**
Yeild = 65-76 %

Conditions ; (a) $SOCl_2$, CH_2Cl_2, reflux, 3 h,
(b) Nucleophile, NEt_3, CH_2Cl_2, 0 °C-rt, 1 h

Compound	Nucleophile	R	Yield (%)	IC_{50} (μM)
52	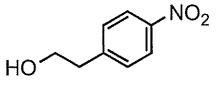	R = $(CH_2)_2p$-$NO_2C_6H_4$	76	2.1
53	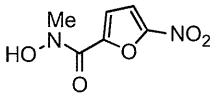	R = 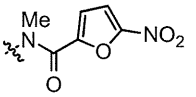	65	2.7

Conditions: (a) $SOCl_2$, CH_2Cl_2, reflux, 3 h; (b) nucleophile, NEt_3, OH_2Ol_2, 0 °C to rt, 1 h.

Table 5
Evaluation of cytotoxicity of the synthesized compounds

Compound	CC_{50} (μM): MT-4	CC_{50} (μM): 293T	Compound	CC_{50} (μM): MT-4	CC_{50} (μM): 293T
1	>100	>100	**29**	–	–
2	>100	>100	**30**	–	–
3	>100	>100	**31**	–	–
4	>100	>100	**32**	–	–
5	>100	>100	**33**	–	–
6	>100	>100	**34**	–	–
7	>100	>100	**35**	–	–
8	>100	>100	**36**	–	–
9	>100	>100	**37**	–	–
10	>100	>100	**38**	–	–
11	>100	67	**39**	–	–
12	–	–	**40**	>100	>100
13	–	–	**41**	–	–
14	>100	>100	**42**	–	–
15	>100	78	**43**	–	–
16	>100	>100	**44**	–	–
17	>100	>100	**45**	–	–
18	>100	>100			
19	–	–	**46**	–	–
20	>100	>100	**47**	–	–
21	71	36	**48**	–	–
22	>100	68	**49**	–	–
23	95	65	**50**	–	–
24	>100	83	**51**	–	–
25	>100	>100	**52**	28	36
26	>100	>100	**53**	86	>100
27	>100	>100			
28	>100	>100			

– means that the measurement for cytotoxicity was not performed because the compound shows no or little inhibitory activity.

coordination force to metal ions is one strategy for increasing inhibitory activity.

RNase H of HIV-1 exerts its enzymatic activity by incorporating divalent metal ions at the reaction site.[26,27] In April 2009, there were 119 entries for the crystal structure of HIV-1 reverse transcriptase in Protein Data Bank. We surveyed the number of divalent metal ions observed at the RNase H domain through all of these 119 crystal structures. As shown in Table S1 in Supplementary data, no metal ion was observed in many of the crystal structures. The presence of Mg^{2+} ions was detected in 16 crystal structures and coordination of Mn^{2+} ions was observed in five structures. Mn^{2+} ion is often used in protein crystallization, because the coordination force to the active site becomes strong with change from Mg and Mn. A single metal ion is observed in most metal-bound crystal structures. Double coordination of divalent metal ions was observed only in 1RTD[28] at that time point. Accordingly, it had been controversial how many metal ions were required at the RNase H reaction site to exert its enzymatic activity.[18,29] A theoretical study by De Vivo et al. suggested that the presence of two divalent metal ions is essential for RNase H activity and that two metal ions act cooperatively with facilitating nucleophilic binding of a substrate and stabilizing the transition state for the enzymatic reaction.[30] De Vivo et al. also suggested that there is a difference in role of those two metal ions. One of the ions is stably bound to the

RNase H active site with an ideal octahedral coordination through the reaction, while the other is slightly irregular with changing the coordination bond. This theoretical finding strongly suggests double coordination of divalent metal ions at the RNase H domain, but the number of coordinated metal ions was still not clearly determined when an RNase H inhibitor was bound to the active site.

From the latter half of 2009, crystal structures on the complex of the RNase H domain and its inhibitor were successively reported from three different research groups.[6–8] All of the crystal structures in the reports showed the presence of two metal ions at the active site. One of the divalent metal ions was held deep inside the binding pocket of the RT RNase H domain with making coordination bonds to three carboxyl groups of Asp443, Glu478 and Asp498. The other was fixed with making coordination bonds to two carboxyl groups of Asp443 and Asp549. The distance between two metal ions was about 4 Å. Every inhibitor in crystal structures was revealed to have a similar binding mode. That is, inhibitors are stabilized with forming coordination bonds to both metal ions.

In the X-ray crystallographic study by Kirschberg et al.[6] the crystallization was archived using the isolated RNase H domain. The inhibitor was a kind of pyrimidinol carboxylic acid derivative. This compound bears a pyrimidine ring connected to one carboxyl group and two hydroxyl groups. This chemical structure shows a significant feature of negatively charged functional groups being aligned in a straight form. This negatively charged region is strongly attached to two divalent metal ions. An oxygen atom located at the center of the straightly aligned polar atoms is positioned between the two metal ions. In their study, many chemical structures were examined by modulating the substitute located at the position opposite the straightly aligned negatively charged atoms on the pyrimidine ring. IC_{50} values of the derivatives were ranged from 0.1 to 70 μM. In their crystal structure; PDB code: 3HYF, the inhibitor has a dichlorobenzyl group as a substitute at the opposite region on the pyrimidine ring. This region was demonstrated to stick out from the binding pocket and to be exposed to the solvent.

An X-ray crystallographic study by Himmel et al.[7] was performed using a protein expressed by RT69A vector. The protein consists of the RT p66 subunit containing F160S and C280S mutations and the p51 subunit containing C280S mutation and truncated at residue 428. The *apo*-crystal without an inhibitor using this protein was reported to give a high-resolution X-ray diffraction.[20] The X-ray analysis by Himmel et al. is the first report for co-crystallization of whole RT and an RNase H inhibitor. The inhibitor was β-thujaplicinol, which shows a high level of RNase H inhibitory activity.[16] β-Thujaplicinol has a unique chemical structure, in which two hydroxyl groups and one carbonyl group are connected to the adjacent three carbon atoms on a seven-member ring. Those negatively charged oxygen atoms are also aligned in a straight form in a manner similar to that for pyrimidinol carboxylic acids. These negatively charged atoms are strongly coordinated to two divalent metal ions. All of the charged atoms are located on one side of the seven-member ring and the oxygen atom positioned at the center of the three aligned negatively charged atoms is coordinated to both metal ions. An alkyl chain is connected to the region opposite to the three negatively charged atoms on the seven-member ring in β-thujaplicinol. In the X-ray crystal structure; PDB code: 3IG1, this alkyl chain was demonstrated to be located outside the binding pocket and exposed to the solvent.

Su et al. also provided X-ray crystal structures on the complex of full-length HIV-1 RT and chemical compounds showing RNase H inhibitory activity.[8] The chemical compounds have a structural basis of pyridine hetero-rings to which one hydroxyl group and one carbonyl group are connected. IC_{50} values of those pyridine heteroring-based derivatives were reported to be 0.1–0.2 μM. The chemical structure also shows a common feature of negatively charged atoms being aligned in a straight form. This negatively charged region was strongly bound to two divalent metal ions. The oxygen atom located at the center of the straightly aligned polar atoms was positioned between the two metal ions. Ethoxy or cyclo-pentane groups are attached to the side opposite the negatively charged region on the hetero-rings. These groups were also shown to stick out from the binding pocket and to be exposed to the solvent in the crystal structures; PDB codes: 3LP0 and 3LP1.

The above three X-ray crystal analyses have revealed that the RNase H active site holds two divalent metal ions and that an RNase H inhibitor is bound to the active site with forming coordination bonds to these metal ions. Accordingly, it is highly probable that the chemical compounds showing RNase H inhibitory activity examined in this study are also coordinated to two divalent metal ions. These compounds have a structural core of nitro-furan and bear an ester linkage at the site opposite the nitro group on the furan ring. Hence, negatively charged oxygen atoms of the nitro group, furan, and carbonyl group are aligned in a straight form. This negatively charged region will be attached to the divalent metal ions.

In order to examine whether the binding mode described in the above paragraph is stable or not, theoretical calculation with QM/MM method was performed. Geometry of the QM region was optimized in the B3LYP/6-31G(d,p) level and that for the MM region was optimized by molecular mechanics approach with the universal force field. All of the atoms were allowed to move freely during geometry optimization. The X-ray crystal structure; PDB code: 3HYF,[6] was used for the computational model for the RNase H domain. The initial atom coordinates before geometry optimization were set to the same as those of the crystal structure. The inhibitor, two Mg^{2+} ions, and side chains of Asp443, Glu478, Asp498, Asp549 and His 539 were assigned to the atoms in the QM region. QM/MM calculations were executed using three kinds of chemical compounds; **3**, **7** and **10**. The dashed lines in Table 1 separate the compounds into several groups in terms of chemical structure, and compounds; **3**, **7** and **10**, bear a typical chemical structure of each group. The inhibitory activity of these compounds is high and the mass-weight is relatively low compared to other chemicals in the same group. Therefore, these compounds will be a basis for our next study. In every optimized structure, the nitro-furan group was shown to be stably bound to two Mg^{2+} ions as shown in Figure 2. The oxygen atom on the furan ring is also oriented toward the divalent metals, while the coordination force seems weak. Carbonyl oxygen at the ester linkage connecting to the furan ring is strongly coordinated to Mg^{2+} ion. Therefore, a large ring-shaped configuration of –O–C–N–O–Mg–Mg–O–C–C– is formed. In compound **3**, the inter-atomic distance of the two Mg^{2+} ions is 4.4 Å. The distance between the nitro-oxygen atom and one Mg^{2+} ion is 2.3 Å, and that between carbonyl oxygen and the other Mg^{2+} ion is 2.2 Å. The pentyl group positioned at the opposite side of the compound sticks out from the binding pocket. Hence, there is much room for improvement in this hydrophobic region. The oxygen atom at the amide bond has a noticeable interaction with the hydroxyl group of Ser499 of the RNase H domain. In compound **7**, the distance between the two Mg^{2+} ions is 3.8 Å. The distance between the nitro-oxygen and one Mg^{2+} ion is 2.0 Å, and that between carbonyl oxygen and the other Mg^{2+} ion is 2.1 Å. The polar atoms composing the amide bond have an interaction with the RNase H domain. In compound **10**, the distance between the two Mg^{2+} ions is 4.3 Å. The distance between nitro-oxygen and one Mg^{2+} ion is 2.1 Å, and that between carbonyl oxygen and the other Mg^{2+} ion is 2.3 Å. The oxygen atom at the amide bond has an interaction with Ser499 of the RNase H domain, while the large hydrophobic moiety at the side part is positioned outside the binding pocket. The QM/MM calculations confirmed that all of the compounds; **3**, **7** and **10**, can be stably bound to the active site of the RNase H domain

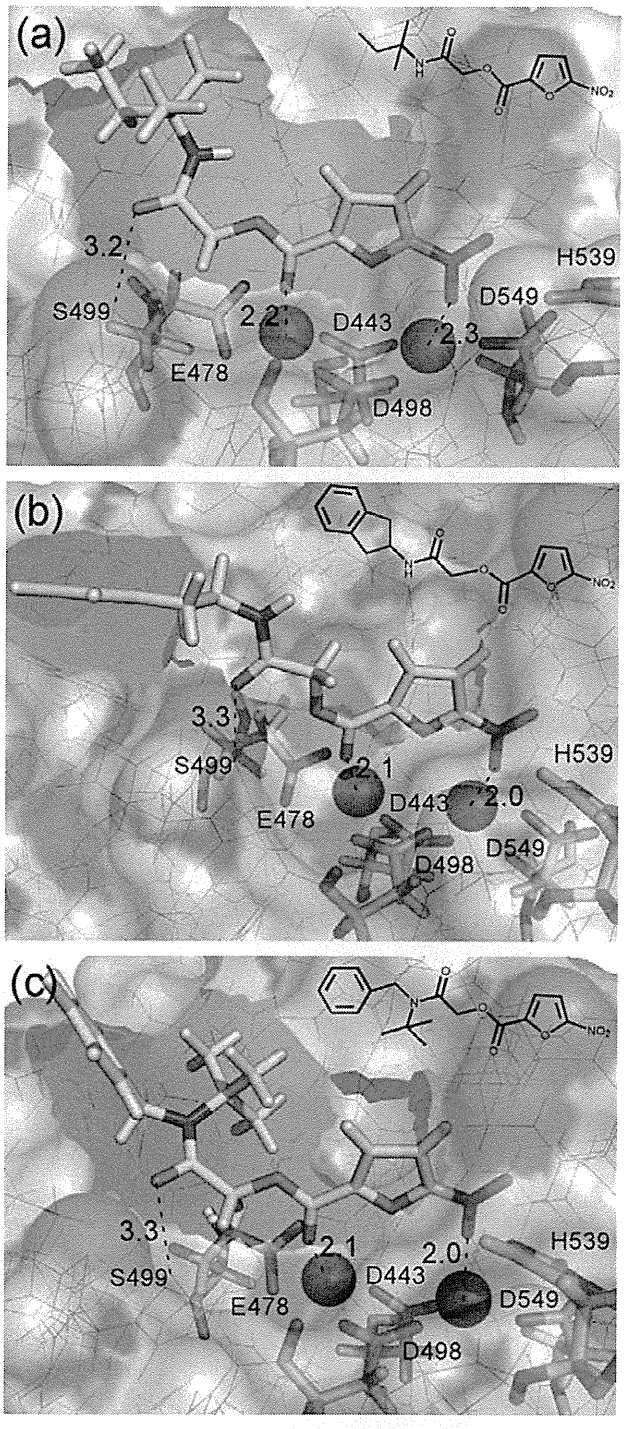

Figure 2. Optimized binding structures of the active compound to the RNase H domain, obtained by QM/MM calculation. (a), (b) and (c) correspond to compounds (**3**), (**7**) and (**10**), respectively. Chemical structures of the compounds are shown at the right top. Inhibitor compound and several polar residues are shown in stick representation. Two Mg^{2+} ions are denoted by spheres. Inter-atomic distances are shown in units of Å.

with coordinating to two divalent metal ions, while the interaction of other moiety is moderate.

Close observation of the optimized geometry by QM/MM calculation indicates that there is some space between the RNase H domain and inhibitory compounds around the ether oxygen at the ester linkage. This suggests that a few water molecules occupy the space when the compounds are bound to the RNase H domain. There exists a polar residue, Ser499, deep inside at this space on the RNase H domain. This residue would have little influence on the function of RNase H. Therefore, one of the designs to improve inhibitory activity is to modify the compound to bear some polar functional group that can interact with Ser499. Substitution of ether oxygen with nitrogen or carbon atom to enable the incorporation of a polar functional group is one of the possible conversions of our derivatives to enhance binding affinity to the RNase H domain.

The difficulty in developing an RNase H inhibitor for practical use lies in the specificity and toxicity. In spite of much effort to enhance the inhibitory potency, the 50% inhibitory concentrations of many compounds reported so far are still in the order of sub-micro molar and they often lack sufficient specificity for HIV-1 RT-associated RNase H activity. Most problematically, they sometime display cytotoxicity to mammalian cells. Many previous compounds have shown little inhibitory activity in an in vitro cell culture replication assay. The derivatives synthesized in this work have a scaffold different from that of the previously reported inhibitors. It was shown in our previous study[17] that the inhibitory potency of the hit chemical was highly specific to RNase H of retrovirus and the hit chemical further displayed an inhibitory activity in a cell culture replication assay. The present study showed that our derivatives had little cytotoxicity and that the chemical conversion at a part other than the 5-nitro-furan-2-carboxylic moiety increased the inhibitory activity. Moreover, there is still much room for modulation of the chemical structure. Accordingly, the analogues bearing the scaffold addressed in this study are good candidates for anti-HIV-1 drugs acting on RT-associated RNase H.

5. Summary

RNase H activity of reverse transcriptase is an attractive target of an antiviral agent for HIV-1 that is not yet addressed by currently approved drugs. A series of chemical compounds were synthesized on the basis of a hit chemical found in our previous in vitro screening. Inhibition of RNase H enzymatic activity was measured in a biochemical assay with a real-time fluorescence monitoring technique. Conversion of the nitro-furan group into other chemical structures drastically decreased the inhibitory activity except for nitro-thiophene. This means that the structural basis of nitro-furan is indispensable for inhibitory activity induced by analogues of the hit chemical. No notable change was observed in inhibitory potency when the hydrophobic moiety located at the opposite part of nitro-furan was modulated. This indicates that the modulated region has little interaction with the RNase H domain. Theoretical calculation with QM/MM method suggested the binding mode of the synthesized compounds to RNase H reaction active site. The characteristic property of the nitro-furan group is large electric polarity. Since oxygen atoms are negatively charged, these oxygen atoms will be strongly coordinated to divalent metal ions of the active site. The findings obtained in this work will be informative for designing potent inhibitors of RNase H enzymatic activity.

Acknowledgments

This work was supported by a Health and Labor Science Research Grant for Research on Publicly Essential Drugs and Medical Devices from the Ministry of Health and Labor of Japan. A part of this work was also supported by a Grant-in-Aid for Scientific Research (C) from Japan Society for the Promotion of Science (JSPS). Theoretical calculations were performed at the Research Center for Computational Science, Okazaki, Japan and at the Information Technology Center of the University of Tokyo and also by the high-performance computer system at Institute for Media Information Technology in Chiba University.

Supplementary data

Supplementary data associated with this article can be found, in the online version, at doi:10.1016/j.bmc.2010.12.011.

References and notes

1. Sarafianos, S. G.; Das, K.; Hughes, S. H.; Arnold, E. *Curr. Opin. Struct. Biol.* **2004**, *14*, 716.
2. Klumpp, K.; Mirzadegan, T. *Curr. Pharm. Des.* **2006**, *12*, 1909.
3. Borkow, G.; Fletcher, R. S.; Barnard, J.; Arion, D.; Motakis, D.; Dmitrienko, G. I.; Parniak, M. A. *Biochemistry* **1997**, *36*, 3179.
4. Tramontano, E.; Esposito, F.; Bads, R.; Di Santo, R.; Costi, R.; La Colla, P. *Antiviral Res.* **2005**, *65*, 117.
5. Tarrago-Litvak, L.; Andreola, M. L.; Fournier, M.; Nevinsky, G. A.; Parissi, V.; de Soultrait, V. R.; Litvak, S. *Curr. Pharm. Des.* **2002**, *8*, 595.
6. Kirschberg, T. A.; Balakrishnan, M.; Squires, N. H.; Barnes, T.; Brendza, K. M.; Chen, X.; Eisenberg, E. J.; Jin, W.; Kutty, N.; Leavitt, S.; Liclican, A.; Liu, Q.; Liu, X.; Mak, J.; Perry, J. K.; Wang, M.; Watkins, W. J.; Lansdon, E. B. *J. Med. Chem.* **2009**, *52*, 5781.
7. Himmel, D. M.; Maegley, K. A.; Pauly, T. A.; Bauman, J. D.; Das, K.; Dharia, C.; Clark, A. D., Jr.; Ryan, K.; Hickey, M. J.; Love, R. A.; Hughes, S. H.; Bergqvist, S.; Arnold, E. *Structure* **2009**, *17*, 1625.
8. Su, H. P.; Yan, Y.; Prasad, G. S.; Smith, R. F.; Daniels, C. L.; Abeywickrema, P. D.; Reid, J. C.; Loughran, H. M.; Kornienko, M.; Sharma, S.; Grobler, J. A.; Xu, B.; Sardana, V.; Allison, T. J.; Williams, P. D.; Darke, P. L.; Hazuda, D. J.; Munshi, S. *J. Virol.* **2010**, *84*, 7625.
9. Moelling, K.; Schulze, T.; Diringer, H. *J. Virol.* **1989**, *63*, 5489.
10. Loya, S.; Hizi, A. *J. Biol. Chem.* **1993**, *268*, 9323.
11. Tan, C. K.; Civil, R.; Mian, A. M.; So, A. G.; Downey, K. M. *Biochemistry* **1991**, *30*, 4831.
12. Davis, W. R.; Tomsho, J.; Nikam, S.; Cook, E. M.; Somand, D.; Peliska, J. A. *Biochemistry* **2000**, *39*, 14279.
13. Himmel, D. M.; Sarafianos, S. G.; Dharmasena, S.; Hossain, M. M.; McCoy-Simandle, K.; Ilina, T.; Clark, A. D., Jr.; Knight, J. L.; Julias, J. G.; Clark, P. K.; Krogh-Jespersen, K.; Levy, R. M.; Hughes, S. H.; Parniak, M. A.; Arnold, E. *ACS Chem. Biol.* **2006**, *1*, 702.
14. Shaw-Reid, C. A.; Munshi, V.; Graham, P.; Wolfe, A.; Witmer, M.; Danzeisen, R.; Olsen, D. B.; Carrol, S. S.; Embrey, M.; Wai, J. S.; Miller, M. D.; Cole, J. L.; Hazuda, D. J. *J. Biol. Chem.* **2003**, *278*, 2777.
15. Hang, J. Q.; Rajendran, S.; Yang, Y.; Li, T.; In, P. W. K.; Overton, H.; Parkes, K. E. B.; Cammack, N.; Martin, J. A.; Klumpp, K. *Biochem. Biophys. Res. Commun.* **2004**, *317*, 321.
16. Budihas, S. R.; Gorshkova, I.; Gaidamakov, S.; Wamiru, A.; Bona, M. K.; Parniak, M. A.; Crouch, R. J.; McMahon, J. B.; Beutler, J. A.; Le Grice, S. F. *Nucleic Acids Res.* **2005**, *33*, 1249.
17. Fuji, H.; Urano, E.; Futahashi, Y.; Hamatake, M.; Tatsumi, J.; Hoshino, T.; Morikawa, Y.; Yamamoto, N.; Komano, J. *J. Med. Chem.* **2009**, *52*, 1380.
18. Davies II, J. F.; Hostomska, Z.; Hostomsky, Z.; Jordan, S. R.; Matthews, D. A. *Science* **1991**, *252*, 88.
19. Klumpp, K.; hang, J. Q.; Rajendran, S.; Yang, Y.; Derosier, A.; Wong Kai In, P.; Overton, H.; Parkes, K. E.; Cammack, N.; Martin, J. A. *Nucleic Acids Res.* **2003**, *31*, 6852.
20. Bauman, J. D.; Das, K.; Ho, W. C.; Baweja, M.; Himmel, D. M.; Clark, A. D., Jr.; Oren, D. A.; Boyer, P. L.; Hughes, S. H.; Shatkin, A. J.; Arnold, E. *Nucleic Acids Res.* **2008**, *36*, 5083.
21. Parniak, M. A.; Min, K. L.; Budihas, S. R.; Le Grice, S. F.; Beutler, J. A. *Anal. Biochem.* **2003**, *322*, 33.
22. Chan, K. C.; Budihas, S. R.; Le Grice, S. F.; Parniak, M. A.; Crouch, R. J.; Gaidamakov, S. A.; Isaaq, H. J.; Wamiru, A.; McMahon, J. B.; Beutler, J. A. *Anal. Biochem.* **2004**, *331*, 296.
23. Li, H.; Robertson, A. D.; Jensen, J. H. *Proteins* **2005**, *61*, 704.
24. Vreven, T.; Morokuma, K.; Farkas, Ö.; Schlegel, H. B.; Frisch, M. J. *J. Comp. Chem.* **2003**, *24*, 760.
25. Frisch, M. J.; Trucks, G. W.; Schlegel, H. B.; Scuseria, G. E.; Robb, M. A.; Cheeseman, J. R.; Montgomery, J. A., Jr.; Vreven, T.; Kudin, K. N.; Burant, J. C.; Millam, J. M.; Iyengar, S. S.; Tomasi, J.; Barone, V.; Mennucci, B.; Cossi, M.; Scalmani, G.; Rega, N.; Petersson, G. A.; Nakatsuji, H.; Hada, M.; Ehara, M.; Toyota, K.; Fukuda, R.; Hasegawa, J.; Ishida, M.; Nakajima, T.; Honda, Y.; Kitao, O.; Nakai, H.; Klene, M.; Li, X.; Knox, J. E.; Hratchian, H. P.; Cross, J. B.; Bakken, V.; Adamo, C.; Jaramillo, J.; Gomperts, R.; Stratmann, R. E.; Yazyev, O.; Austin, A. J.; Cammi, R.; Pomelli, C.; Ochterski, J. W.; Ayala, P. Y.; Morokuma, K.; Voth, G. A.; Salvador, P.; Dannenberg, J. J.; Zakrzewski, V. G.; Dapprich, S.; Daniels, A. D.; Strain, M. C.; Farkas, O.; Malick, D. K.; Rabuck, A. D.; Raghavachari, K.; Foresman, J. B.; Ortiz, J. V.; Cui, Q.; Baboul, A. G.; Clifford, S.; Cioslowski, J.; Stefanov, B. B.; Liu, G.; Liashenko, A.; Piskorz, P.; Komaromi, I.; Martin, R. L.; Fox, D. J.; Keith, T.; AlLaham, M. A.; Peng, C. Y.; Nananyakkara, A.; Challacombe, M.; Gill, P. M. W.; Johnson, B.; Chen, W.; Wong, M. W.; Gonzalez, C.; Pople, J. A. GAUSSIAN 03; Gaussian, Inc.: Wallingford, CT, 2004.
26. Smith, J. S.; Roth, M. J. *J. Virol.* **1993**, *67*, 4037.
27. Sarafianos, S. G.; Das, K.; Tantillo, C.; Clark, A. D., Jr.; Ding, J.; Whitcomb, J. M.; Boyer, P. L.; Hughes, S. H.; Arnold, E. *EMBO J.* **2001**, *20*, 1449.
28. Huang, H.; Chopra, R.; Verdine, G. L.; Harrison, S. C. *Science* **1998**, *282*, 1669.
29. Katayanagi, K.; Okumura, M.; Morikawa, K. *Proteins* **1993**, *17*, 337.
30. De Vivo, M.; Dal Peraro, M.; Klein, M. L. *J. Am. Chem. Soc.* **2008**, *130*, 10955.